CORE
Metadata, citation and similar papers at core.ac.uk
Provided by Elsevier - Publisher Connector

Current Biology 17, 1913–1924, November 20, 2007 ©2007 Elsevier Ltd All rights reserved DOI 10.1016/j.cub.2007.10.045

Article

A Novel Requirement for *C. elegans* Alix/ALX-1 in RME-1-Mediated Membrane Transport

Anbing Shi,[1] Saumya Pant,[1] Zita Balklava,[1] Carlos Chih-Hsiung Chen,[1] Vanesa Figueroa,[1] and Barth D. Grant[1,*]
[1]Department of Molecular Biology and Biochemistry
Rutgers University
Piscataway, New Jersey 08854

Summary

Background: Alix/Bro1p family proteins have recently been identified as important components of multivesicular endosomes (MVEs) and are involved in the sorting of endocytosed integral membrane proteins, interacting with components of the ESCRT complex, the unconventional phospholipid LBPA, and other known endocytosis regulators. During infection, Alix can be co-opted by enveloped retroviruses, including HIV, providing an important function during virus budding from the plasma membrane. In addition, Alix is associated with the actin cytoskeleton and might regulate cytoskeletal dynamics.
Results: Here we demonstrate a novel physical interaction between the only apparent Alix/Bro1p family protein in *C. elegans*, ALX-1, and a key regulator of receptor recycling from endosomes to the plasma membrane, called RME-1. The analysis of *alx-1* mutants indicates that ALX-1 is required for the endocytic recycling of specific basolateral cargo in the *C. elegans* intestine, a pathway previously defined by the analysis of *rme-1* mutants. The expression of truncated human Alix in HeLa cells disrupts the recycling of major histocompatibility complex class I, a known Ehd1/RME-1-dependent transport step, suggesting the phylogenetic conservation of this function. We show that the interaction of ALX-1 with RME-1 in *C. elegans*, mediated by RME-1/YPSL and ALX-1/NPF motifs, is required for this recycling process. In the *C. elegans* intestine, ALX-1 localizes to both recycling endosomes and MVEs, but the ALX-1/RME-1 interaction appears to be dispensable for ALX-1 function in MVEs and/or late endosomes.
Conclusions: This work provides the first demonstration of a requirement for an Alix/Bro1p family member in the endocytic recycling pathway in association with the recycling regulator RME-1.

Introduction

The endocytic pathway of eukaryotes is essential for the internalization and trafficking of macromolecules, fluid, membranes, and membrane proteins. Membrane-associated receptors and ligands are endocytosed either through clathrin-dependent or clathrin-independent uptake mechanisms [1, 2]. After the cargo is sorted in early endosomes, some cargo is transported from early to late endosomes and eventually to lysosomes for degradation [3]. Other cargo types recycle to the plasma membrane either directly, or indirectly via recycling endosomes [3, 4]. Studies in HeLa cells indicate that receptors internalized via clathrin-dependent and clathrin-independent mechanisms meet in the endosomal system but then recycle to the cell surface in distinct carriers [5].

In recent years, it has become clear that Alix/Bro1p family proteins are conserved components of endosomal transport pathways. Alix and Bro1p are thought to function in the multivesicular endosome (MVE) pathway, promoting the degradation of integral membrane proteins [6, 7]. Multivesicular endosomes contain lumenal vesicles formed by the inward invagination of the limiting membrane, and they likely represent intermediates in the maturation of the pleiomorphic early endosomes into late endosomes [8]. Membrane proteins sorted into the lumenal vesicles of MVEs are degraded upon the fusion of the MVEs with lysosomes in metazoans and with the vacuole in yeast [9]. The sorting of cargo, and the budding of vesicles into the lumen of the MVE, depends on a network of proteins organized into four major hetero-oligomeric complexes and several monomeric or homo-oligomeric proteins: the Vps27/Hse1 complex (Hrs/STAM in humans), ESCRT-I, II, and III, the AAA ATPase Vps4, the ubiquitin hydrolase Doa4p, and Alix/Bro1p.

Alix and Bro1p contain a conserved ~380 amino acid Bro1 domain near their N termini [10, 11]. Alix/Bro1p also contains a central V domain (aa 362–702 in Alix) consisting of two extended three-helix bundles and a conserved C-terminal proline-rich domain (PRD) [12]. The Bro1 domain is necessary for the endosomal localization of Alix/Bro1p and mediates membrane association through binding to the ESCRT-III complex subunit Snf7p/CHMP4b [6, 13–15]. The PRD of Alix interacts with a number of endocytic regulatory proteins, including SETA [16], endophilins [17], and the ESCRT-I complex subunit Tsg101 [18, 19].

Through the second arm of its V domain, Alix also interacts with HIV-1 Gag and other retroviral proteins containing the motif tyrosine-proline-X-leucine (YPXL), promoting the budding of viral particles from the plasma membrane [12, 18–20]. Likewise, the Aspergillus Alix homolog PalA interacts with the PacC protein through YPXL motifs [21]. In vitro Alix is preferentially recruited by liposomes containing the phospholipid 2,2′ lysobisphosphatidic acid (LBPA) [22]. LBPA is enriched in the internal membranes of MVEs and possesses the capacity to drive the formation of membrane invaginations within acidic liposomes [22]. It has been suggested that Alix is a target for this important lipid, potentially regulating the invagination process or back fusion of internal vesicles with the limiting membrane [22]. Alix also associates with structural proteins of the cytoskeleton, especially actin [23, 24], and is important for the actin-dependent intracellular positioning of endosomes, and the formation of stress fibers, in tissue culture cells [23, 25].

*Correspondence: grant@biology.rutgers.edu

We and others have previously established in vivo endocytic assay systems for the genetic analysis of trafficking in *C. elegans* tissues [26–29]. Among the endocytic regulators found in our screens, we identified RME-1 [30]. *rme-1* mutants display endocytic recycling defects in several tissues [30], including the strongly reduced uptake of yolk proteins by oocytes, due to poor recycling of yolk receptors, reduced uptake of fluid-phase markers by coelomocytes, and the accumulation of gigantic fluid-filled recycling endosomes in the intestinal cells, due to defective recycling of basolaterally endocytosed pseudocoelomic fluid. Evidence from studies of mammalian Ehd1/mRme-1 also indicates a function in recycling, specifically in the exit of membrane proteins from recycling endosomes [31]. All members of the RME-1 family contain a C-terminal eps15 homology (EH) domain [30, 32]. The EH domain is associated with endocytic transport in mammalian cells and yeast [33, 34]. Previous studies showed that the EH domain of RME-1 homologs, and that of other EH domain proteins, interacts with target proteins through specific binding to sequences containing asparagine-proline-phenylalanine (NPF) motifs [32, 33, 35]. In mammals, RME-1/Ehd1 forms protein complexes with syndapin through EH-NPF interactions, which is important for recycling endosome function [36].

Here, we show that *C. elegans* ALX-1 is physically associated with both recycling endosomes and MVEs and provide evidence that ALX-1 functions with RME-1 in the *C. elegans* intestine, promoting the recycling of basolateral cargo internalized independently of clathrin. This endocytic recycling regulation requires the RME-1/ALX-1 interaction and is specifically mediated by RME-1-YPSL and ALX-1-NPF motifs.

Results

Physical Association of ALX-1 and RME-1

In order to identify new regulators of endocytic recycling, we performed a yeast two-hybrid screen for binding partners of RME-1 by using the C-terminal region of RME-1 including the EH domain (isoform D, amino acids 442–576) as bait. This screen identified several interacting clones encoding ALX-1, the *C. elegans* ortholog of human Alix/AIP1 and yeast Bro1p (Figure 1 and the Supplemental Experimental Procedures in the Supplemental Data available online). We confirmed the binding interaction by using an in vitro glutathione S-transferase (GST)-pulldown assay (Figure S1, as indicated). The novel interaction that we detected between ALX-1 and the recycling endosome protein RME-1 suggested that ALX-1 might function on recycling endosomes, in addition to MVEs, or that RME-1 has a previously undetected function in the MVE.

To clarify interaction domains within RME-1 and ALX-1, we tested a series of truncated versions of the proteins in the two-hybrid assay. This analysis identified two modes of binding between the two proteins. First we noted that the extreme C terminus of RME-1, just after the EH domain, contains a tyrosine-proline-X-leucine (YPSL) motif, similar to that used by mammalian Alix to bind to retroviral Gag proteins [37] and that used by Aspergillus PalA to bind to PacC [21]. The central region of ALX-1 from amino acids 365–752 was sufficient to mediate

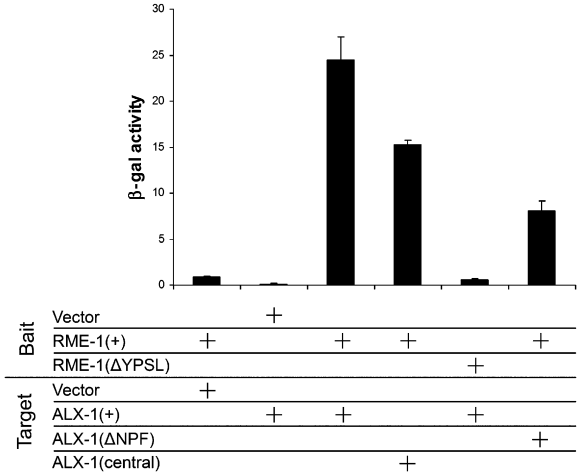

Figure 1. RME-1 Interacts with ALX-1

Quantitative yeast two-hybrid β-galactosidase (β-gal) assays show that the ALX-1 C-terminal NPF motif contributes to the interaction with RME-1, whereas the central domain (aa 365–752) of ALX-1 contributes the main binding surface, interacting with RME-1 through its C-terminal YPSL sequence. The y axis is labeled in Miller units.

the interaction, and the deletion of the final nine amino acids of RME-1 including the YPSL sequence completely abrogated the interaction. In addition, we noted that the extreme C terminus of ALX-1 contains an asparagine-proline-phenylalanine tripeptide motif. The EH domain of RME-1 homologs, and other EH-domain proteins, are known to bind to NPF-containing sequences [32, 35]. The deletion of the NPF sequence in the context of the yeast two-hybrid prey construct reduced the RME-1/ALX-1 interaction by almost 3-fold but did not completely block association (Figure 1). The Bro1 domain of ALX-1 was dispensable for the two-hybrid interaction. Taken together, these results suggest that the central domain of ALX-1 contributes the main binding surface, interacting with the C terminus of RME-1 through the YPSL-containing tail, whereas the NPF sequence of ALX-1 interacts with the RME-1 EH domain, perhaps modulating the interactions.

ALX-1 Is Broadly Expressed in *C. elegans*

To determine what tissues express ALX-1 and are thus cell types in which ALX-1 might interact with RME-1 in vivo, we created transgenic animals expressing a GFP-ALX-1 (GFP: green fluorescent protein) translational fusion gene driven by the *alx-1* promoter (see the Supplemental Experimental Procedures). We observed ubiquitous expression of GFP-ALX-1 with notably high levels of expression in the intestine, hypodermis, body-wall muscles, nervous system, spermatheca, coelomocytes, and pharynx (Figures 2A–2F). The GFP-ALX-1 fusion protein appeared punctate in most tissues. In the intestine, GFP-ALX-1 was enriched near the apical plasma membrane (PM) and was also clearly enriched on distinct cytoplasmic puncta (Figure 2A, arrowheads). Intestine-specific expression of equivalent fusions of ALX-1 to GFP or mCherry produced indistinguishable subcellular localization patterns and rescued *alx-1* mutant phenotypes (see below and the Supplemental Experimental Procedures), indicating that the expression

Figure 2. ALX-1 is Broadly Expressed in *C. elegans*

The expression of a GFP-ALX-1 transgene driven by the *alx-1* promoter is indicated in (A–F). Scale bars represent 10 μm.
(A) Intestine. Arrowheads indicate cytoplasmic puncta.
(B) The pharynx is indicated by arrows, and the nerve ring is indicated by arrowheads.
(C) The arrow indicates spermatheca, and the arrowhead indicates cytoplasmic puncta.
(D) Coelomocytes, cytoplasmic puncta (arrowheads).
(E) Nerve cord (arrowheads) and body-wall muscle (arrow).
(F) Hypodermis, cytoplasmic puncta (arrowheads).

pattern and subcellular localization of the reporters very likely reflect those of the endogenous protein.

ALX-1 Is Associated with Recycling Endosomes and MVEs in the Intestine

Because RME-1 and its mammalian homologs have not been found localized to MVEs and are not required for membrane protein degradation but rather are greatly enriched on recycling endosomes and function in recycling, we sought to determine whether ALX-1 protein is present on recycling endosomes. First, we compared the subcellular localization of intestinally expressed mCherry-ALX-1 with GFP-RME-1, which is found on basolateral recycling endosomes [30, 38]. mCherry-ALX-1 colocalized extensively with GFP-RME-1 (Figures 3A–3C). Puncta positive for mCherry-ALX-1 and GFP-RME-1 were more frequent close to the basolateral PM and are best observed in the top focal plane (Figures 3A–3C; Figures S2A–S2D). Fewer ALX-1 and RME-1 double-positive structures were found in the middle focal planes, which offer better views of the medial and apical membranes. These results indicated that ALX-1 is present on basolateral recycling endosomes, where it could interact with RME-1 to regulate recycling. Our results also indicated that ALX-1 is present on other unidentified structures in the intestine. We obtained identical results with the fluorescent tags reversed, comparing GFP-ALX-1 with mCherry-RME-1.

Because mammalian Alix and yeast Bro1p are thought to be associated with MVEs, we also compared the localization of mCherry-ALX-1 with GFP-tagged HGRS-1 [39, 40], the worm ortholog of the MVE protein Hrs/Vps27p. GFP-HGRS-1 mainly colocalized with mCherry-ALX-1 on puncta of the medial and apical cytoplasm (Figures 3D–3F, arrowheads; Figures S2E–S2H). These results suggest that ALX-1 is present on MVEs in addition to recycling endosomes. We confirmed that the RME-1-labeled recycling endosomes and the HGRS-1-labeled MVEs are independent vesicle populations by directly comparing the subcellular localization of GFP-HGRS-1 and mCherry-RME-1. We did not observe any colocalization between GFP-HGRS-1- and mCherry-RME-1-labeled puncta, substantiating this inference (Figures 3G–3I).

We also compared mCherry-ALX-1 with markers for early endosomes (GFP-RAB-5), late endosomes (GFP-RAB-7), and TGN and apical recycling endosomes (GFP-RAB-11) (Figure S3). We observed the occasional colocalization of mCherry-ALX-1 with the early-endosome marker GFP-RAB-5 and did not observe colocalization with the TGN/ARE marker. mCherry-ALX-1 did not clearly label the large ring-like GFP-RAB-7-positive

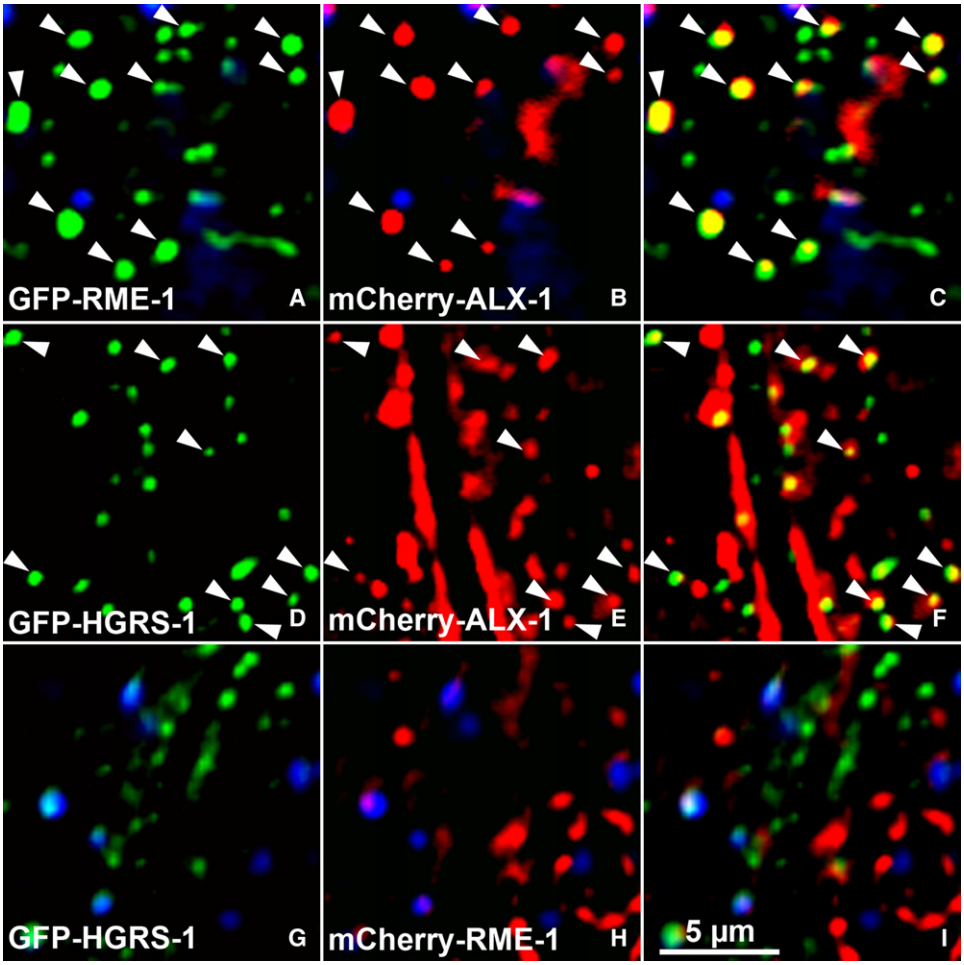

Figure 3. ALX-1 Associates with Two Types of Endosomes in the Intestine

(A–C) mCherry-ALX-1 colocalizes with GFP-RME-1 on basolateral recycling endosomes. Arrowheads indicate endosomes labeled by both GFP-RME-1 and mCherry-ALX-1.

(D–F) Some mCherry-ALX-1 also colocalizes with MVE marker GFP-HGRS-1, mostly in the medial and apical cytoplasm. Arrowheads indicate puncta labeled by both mCherry-ALX-1 and GFP-HGRS-1.

(G–I) mCherry-RME-1 and GFP-HGRS-1 label different endosome types. Virtually no overlap was observed between mCherry-RME-1 and GFP-HGRS-1.

In each image, autofluorescent lysosomes can be seen in all three channels with the strongest signal in blue, whereas GFP appears only in the green channel and mCherry only in the red channel. Signals observed in the green or red channels that do not overlap with signals in the blue channel are considered bona fide GFP or mCherry signals, respectively. The scale bar represents 5 μm.

late endosomes, but some mCherry-ALX-1 puncta appeared on or near the rings. The weak colocalization with early- and late-endosome markers is consistent with the presence of ALX-1 on MVEs because MVEs represent an intermediate in the maturation of early endosomes to late endosomes. Taken together, our results indicate that ALX-1 resides on two independent classes of endosomes in the worm intestine, where it could potentially contribute to membrane traffic.

ALX-1-Positive Structure Number Increases in *rme-1* Mutants

As an additional test of the association of ALX-1 with recycling endosomes, we quantified the number of GFP-ALX-1-positive puncta in an *rme-1*(*b1045*) null mutant background. For comparison, we also assayed GFP-HGRS-1, which is expected to label MVEs but not recycling endosomes. We previously established that *rme-1* mutant intestines specifically accumulate abnormally high numbers of basolateral recycling endosomes but do not accumulate increased numbers of early, late, or apical recycling endosomes [38]. Thus, if ALX-1 is associated with basolateral recycling endosomes, we would expect to observe an increase in GFP-ALX-1 puncta number. *rme-1* null mutant intestines showed a nearly 3-fold increase in GFP-ALX-1 puncta number but no change in GFP-HGRS-1 puncta number (Figures 4B and 4C; Figure S4). These results are entirely consistent with residence of ALX-1 on basolateral recycling endosomes. These results also indicate that ALX-1 association with such endosomes does not require RME-1.

Loss of ALX-1 Results in Intracellular Accumulation of Recycling Cargo

Given the physical association and colocalization of ALX-1 and RME-1, we sought to determine whether the loss of ALX-1 affects basolateral recycling. Toward

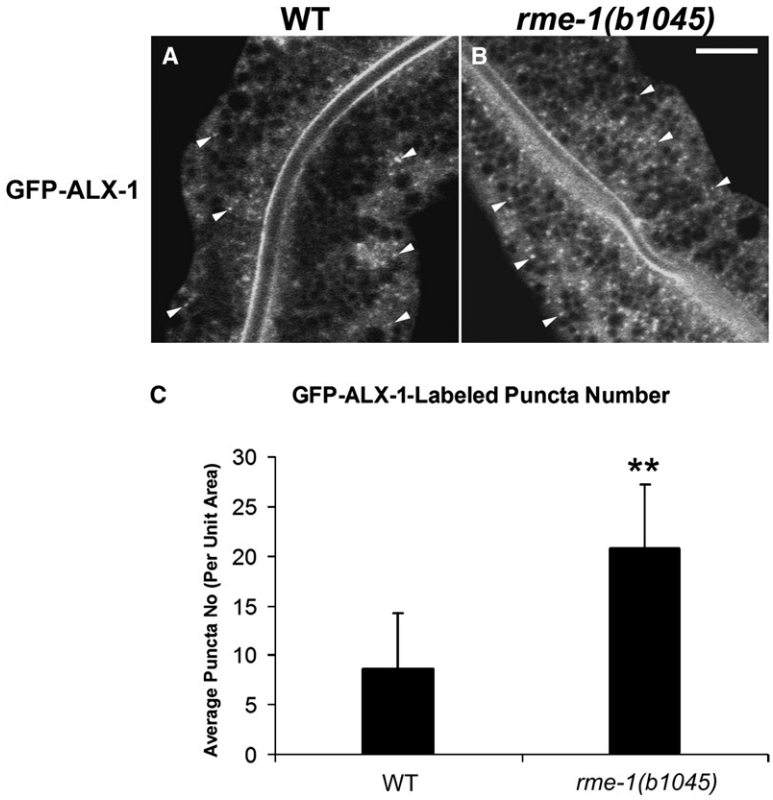

Figure 4. *rme-1* Mutants Accumulate Abnormally Numerous GFP-ALX-1-Labeled Endosomes

(A and B) Confocal images of wild-type animals (A) and *rme-1(b1045)* mutant animals (B) showing GFP-ALX-1-labeled endosomes in the intestine. Arrowheads indicate GFP-ALX-1 puncta. The scale bar represents 10 μm.
(C) Quantification of endosome number in wild-type animals and mutants as visualized by GFP-ALX-1. Error bars represent standard deviations from the mean (n = 18 each, six animals of each genotype sampled in three different regions of each intestine). Asterisks indicate a significant difference in the one-tailed Student's t test ($p < 0.01$).

this end, we obtained a deletion allele of *alx-1*, *gk275*, created by the *C. elegans* Gene Knockout Consortium. This mutation deletes the first exon and part of the second exon and is not predicted to produce any functional ALX-1 protein. *alx-1(gk275)* mutants are viable and at the gross organismal level appeared fairly normal, similar to *rme-1* mutants and several other endocytic trafficking mutants that we have previously examined.

As a first step to determine whether *alx-1* is required for basolateral recycling, we assayed the localization of basolaterally recycling transmembrane cargo proteins at steady state, comparing wild-type animals with *alx-1*(*gk275*) mutant animals. Equivalent GFP fusions for these cargo proteins have previously been shown to be functional and traffic normally in mammalian cells, and we have previously characterized them in the *C. elegans* intestine [38]. First, we assayed for effects on the localization of the α chain of the human interleukin-2 (IL-2) receptor TAC (hTAC-GFP), which is a marker for clathrin-independent uptake and *rme-1*-dependent recycling in mammalian cells [5, 41] and which we have previously shown accumulates extensively in aberrant endosomes in *C. elegans rme-1* mutants [38]. We observed significant aberrant accumulation of hTAC-GFP in cytoplasmic puncta in *alx-1* mutant intestines. hTAC-GFP puncta number was increased by 3-fold in *alx-1* mutants compared to wild-type controls (Figures 5C, 5D, and 5E). These results suggest that the recycling of clathrin-independent cargo requires ALX-1.

We then assayed the human transferrin receptor (hTfR-GFP), which is a marker for clathrin-dependent uptake and *rme-1*-dependent recycling in mammalian cells [31, 42, 43]. We have previously shown that hTfR-GFP accumulates in aberrant endosomes in *C. elegans rme-1* mutants but not as extensively as hTAC-GFP [38]. We could not detect any changes in localization for hTfR-GFP (Figures 5A and 5B), suggesting that clathrin-dependent cargo recycles normally in the absence of ALX-1.

In order to determine whether human Alix is also required for the recycling of clathrin-independent cargo, we analyzed major histocompatibility complex (MHC) class I recycling in HeLa cells by using a previously established pulse-chase assay that follows a non-perturbing anti-MHC class I monoclonal antibody [44]. MHC class I is a well documented marker for clathrin-independent uptake and Ehd1/mRme-1-dependent recycling in mammalian cells [41, 45]. Cells transfected with an mRFP1 control vector were compared to cells cotransfected with mRFP1 and a FLAG-tagged dominant negative form of Alix (Alix-CT [CT: carboxy terminal], amino acids 467–869) [46].

MHC class I uptake was similar between mRFP1-transfected (RFP: red fluorescent protein) cells and mRFP1/FLAG-Alix(467–869) cotransfected cells (Figures 5F, 5G, and 5J). MHC class I recycling in mRFP1/FLAG-Alix(467–869) cotransfected cells was reduced by 12-fold compared to control mRFP1-transfected cells (Figures 5H, 5I, and 5K), suggesting that the requirement for Alix/ALX-1 in this recycling pathway is conserved from worms to mammals.

We also analyzed clathrin-dependent cargo transferrin (Tf) uptake and recycling in HeLa cells by using a previously described assay [47]. EGFP/FLAG-Alix (467–869) cotransfected cells showed slightly reduced, but not statistically different, Alexa568-Tf uptake (84.4% ± 9.8% of control, $p = 0.055$) when compared to control cells transfected with EGFP control plasmid

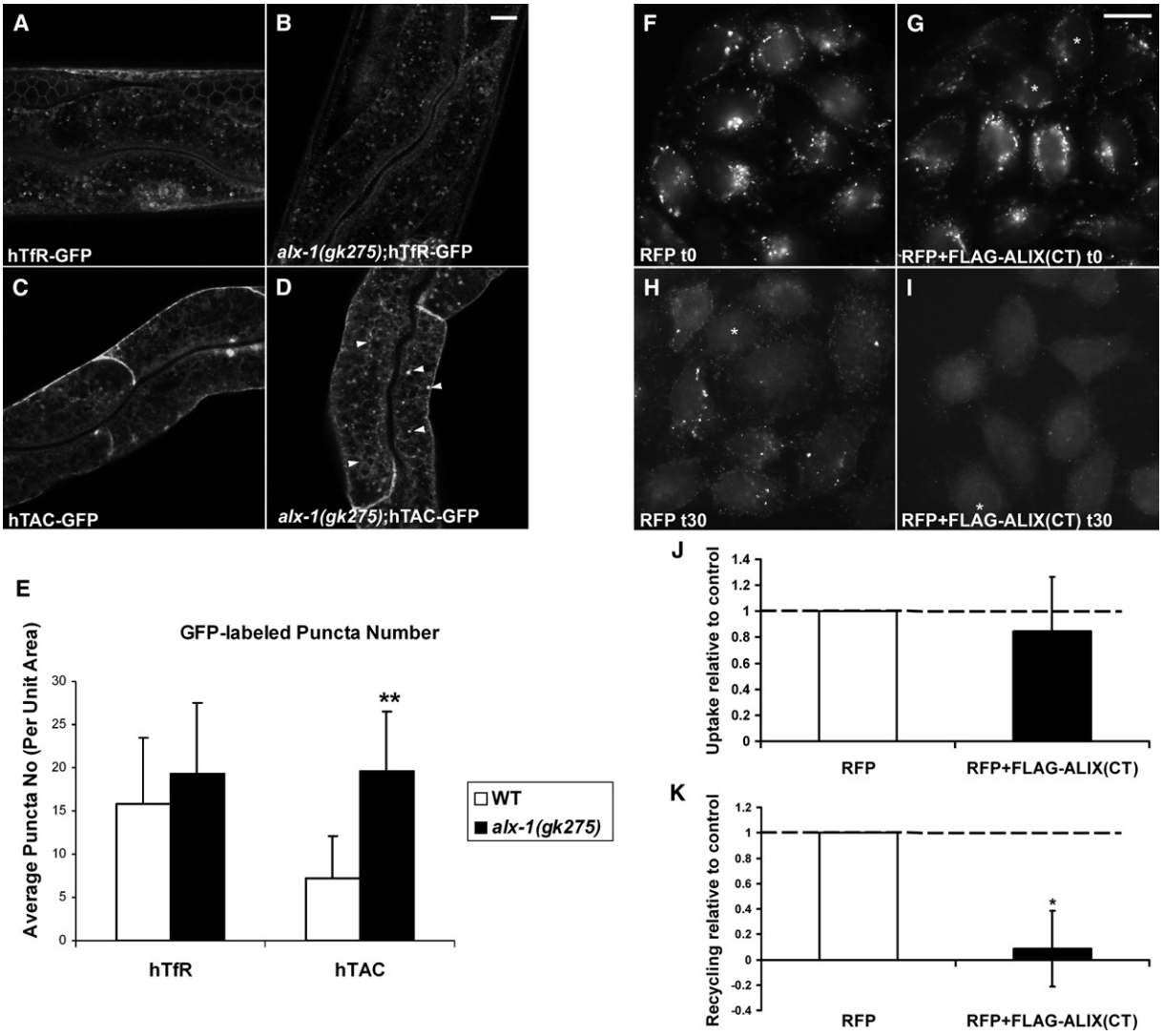

Figure 5. Abnormal Trafficking of Recycling Cargo in *alx-1* Mutant *C. elegans* and in HeLa Cells Expressing Truncated Alix

(A and B) The localization and morphology of hTfR-GFP, a clathrin-dependent cargo protein, appears unchanged in *alx-1(gk275)* mutants compared to wild-type animals. The scale bar represents 10 μm.

(C and D) hTAC-GFP, a cargo protein internalized independently of clathrin, becomes trapped in endosomal structures of *alx-1* mutants. Arrowheads indicate punctate and tubular endosomes labeled by hTAC-GFP in the intestine.

(E) Quantification of cargo-labeled puncta number. Error bars represent standard deviations from the mean (n = 18 each, six animals of each genotype sampled in three different regions of each intestine).

(F–I) Representative images showing anti-MHC class I labeling in control HeLa cells transfected with RFP expression plasmid only (F and H) or for cells cotransfected with RFP and truncated Alix expression plasmids (G and I). The first pair of images (F and G) show anti-MHC class I uptake after 30 min incubation. The second pair of images (H and I) show surface MHC class I after 30 min of recycling. Cells that were negative for the RFP signal are marked with asterisks. In cotransfection experiments, these RFP-negative cells may or may not express Alix(467–869) (see the Supplemental Experimental Procedures) and were therefore not included in the quantification. Conversely, nearly all RFP-expressing cells were found to also express FLAG-Alix(467–869) in control experiments. Therefore, only RFP-expressing cells were quantified for anti-MHC class I uptake or recycling. The scale bar represents 20 μm.

(I–J) The amount of MHC class I antibody internalized after a 30 min pulse, or recycled after a 30 min chase, is shown as a ratio relative to control cells (see the Supplemental Experimental Procedures). MHC class I antibody recycling (K), but not MHC class I antibody uptake (J), was impaired by expression of truncated FLAG-Alix(467–869). The asterisk in (K) indicates a significant difference in the one-tailed Student's t test ($p = 0.004$).

only. There was also no significant difference in the amount of recycled Alexa568-Tf between control EGFP-transfected cells (62.2% ± 15.6%) and EGFP/FLAG-Alix(467–869) cotransfected cells (71.9% ± 13.9%), which is in agreement with previously published data with Alix small interfering RNA (siRNA) [25].

alx-1 Mutants Accumulate Abnormally High Numbers of RME-1-Positive Endosomes

The increased number and size of hTAC-GFP-labeled puncta in *alx-1* mutants suggested a block in hTAC recycling and a concomitant increase in basolateral recycling endosome number and size, similar to the

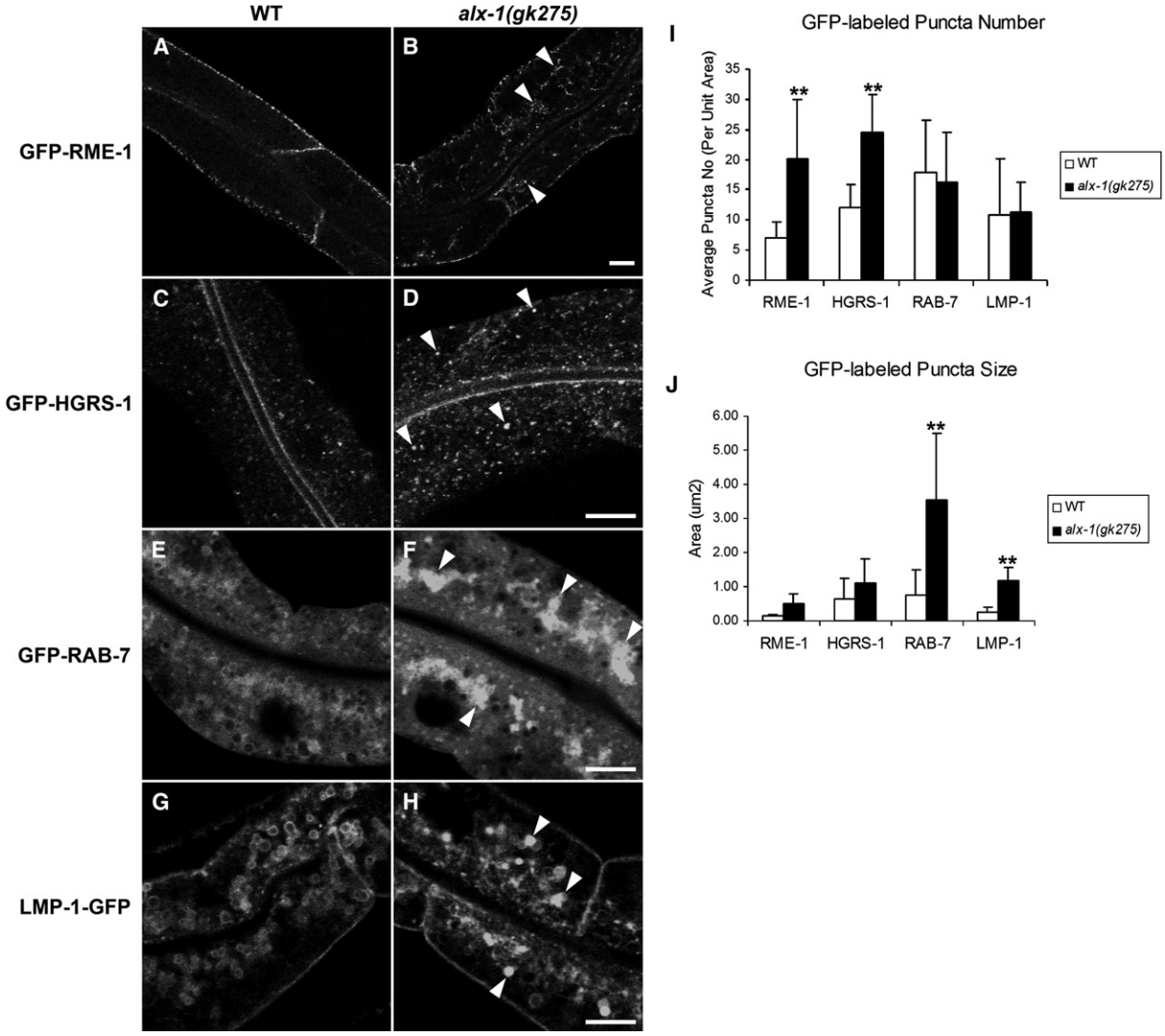

Figure 6. Altered Endosome Populations in *alx-1* Mutants

(A and B) GFP-RME-1-labeled recycling endosomes increase in number in *alx-1* mutant intestinal cells. Arrowheads indicate punctate and tubular endosomes labeled by GFP-RME-1.

(C and D) GFP-HGRS-1-positive endosomes increase in number in *alx-1* mutant intestinal cells. Arrowheads indicate punctate endosomes labeled by GFP-HGRS-1.

(E–H) GFP-RAB-7- and LMP-1-GFP-labeled late endosomes appear enlarged and aggregated in *alx-1(gk275)* mutant intestinal cells.

(I–J) Quantification of GFP-labeled puncta number and puncta size. Error bars represent standard deviations from the mean (n = 18 each, six animals of each genotype sampled in three different regions of each intestine). The asterisks indicate a significant difference in the one-tailed Student's t test ($p < 0.01$).

Scale bars represent 10 μm.

phenotype of *rme-1* mutants [30, 38]. To further analyze the effect of the *alx-1* knockout on recycling-endosome number and size, we quantified the number of GFP-RME-1-labeled endosomes in *alx-1* mutants. In wild-type animals, GFP-RME-1 strongly labels endosomes very near the basolateral PM (Figure 6A). GFP-RME-1 also weakly labels structures very near the apical PM that could be apical recycling endosomes [38]. In *alx-1* mutants, an abnormally large number of GFP-RME-1-labeled endosomes accumulated, most notably appearing in large numbers throughout the cytoplasm in addition to the normally localized cortical structures (Figure 6B). Image quantitation revealed an approximately 3-fold increase in GFP-RME-1 puncta number and size (Figures 6I and 6J). No defects were found in the localization of an apical recycling-endosome- and TGN-associated marker, GFP-RAB-11, in the intestine of *alx-1* mutants (Figure S5). These results suggest that ALX-1 is important for the normal function of RME-1-positive basolateral recycling endosomes and taken together with the effects on hTAC-GFP accumulation in worms, and MHC class I recycling in HeLa cells, suggest that ALX-1/Alix is important for the efficient export of certain cargo proteins from recycling endosomes. These results also indicate that ALX-1 is not required for the association of RME-1 with endosomes, suggesting that ALX-1 affects RME-1 function rather than its recruitment.

SDPN-1 Recruitment to Basolateral Endosomes Fails in *alx-1* Mutants

The F-Bar and SH3 domain protein syndapin is a regulator of endocytic transport and actin dynamics. Previous work in HeLa cells showed that syndapin is a binding partner of mammalian Ehd1/mRme-1 on recycling endosomes and functions with Ehd1/mRme-1 in recycling [36]. This lead us to test whether syndapin is also involved in the basolateral recycling pathway described here. *C. elegans* has a single ortholog of syndapin, called SDPN-1, and we found that SDPN-1-GFP expressed from its own promoter is highly expressed in the intestine and colocalizes with RME-1 on basolateral recycling endosomes (data not shown). Further analysis showed that *alx-1* mutants lack SDPN-1 on basolateral structures, implying an inability to recruit SDPN-1 to basolateral endosomes (Figures 7B and 7H). In *rme-1* mutants, basolateral SDPN-1-GFP-labeled structures were also significantly altered, characterized by loss of most basolateral SDPN-1-GFP-labeled structures and with many of the remaining structures appearing greatly enlarged (Figures 7C and 7F). *alx-1* mutant animals depleted of RME-1 by RNA interference (RNAi) displayed a mixed phenotype, with weaker SDPN-1-GFP labeling of endosomes that appeared to be enlarged, but less enlarged than in animals lacking RME-1 only (Figures 7C and 7D). Apical SDPN-1 appeared normally localized in *alx-1* and *rme-1* mutants. Because syndapin regulates membrane-associated actin dynamics and promotes membrane tubulation, the failure of basolateral recycling endosomes to recruit SDPN-1 to basolateral recycling endosomes might be the primary defect resulting in intracellular accumulation of recycling cargo in *alx-1* mutants.

MVE and Late-Endosome Morphology Is Aberrant in *alx-1* Mutants

Analysis in early embryos indicated that ALX-1 is required for the degradation of integral membrane proteins (see the Supplemental Results and Figures S6A–S6D), a process that does not require RME-1 but does require ESCRT proteins [48]. To assay for changes in the MVE and/or late-endosome pathway in the intestine, we performed endosome morphometric analysis of *alx-1* mutant animals. We did not observe any effect of the loss of ALX-1 on RAB-5-positive early-endosome number or size (Figure S5). Consistent with a role for ALX-1 in intestinal MVE function, we found a 2-fold increase in MVE number and size in *alx-1* mutants in GFP-HGRS-1-expressing strains (Figures 6D, 6I, and 6J). We also observed a dramatic effect on GFP-RAB-7- and LMP-1-GFP-positive late endosomes, which accumulated in normal numbers but which displayed grossly abnormal morphology (Figures 6F and 6H), with an average 5-fold increase in late-endosome size (Figure 6J). Consistent with our cargo analysis in *alx-1* mutant embryos, these results indicate that MVE and late-endosome morphology, and likely their functions, require ALX-1 in vivo.

Basolateral Recycling Endosomes Require the Interaction of RME-1 with ALX-1

Finally, we sought to specifically test the role of the RME-1/ALX-1 interaction in transport, as opposed to the roles of the individual proteins. We accomplished this by reintroducing interaction-defective forms of RME-1 or ALX-1 into their cognate null mutants and assaying for rescue of the loss-of-function phenotypes.

Our yeast two-hybrid studies indicated that RME-1 C-terminal tail containing the YPSL motif is required for RME-1 to bind to ALX-1. To determine the importance of the YPSL tail in vivo and the contribution of ALX-1 binding to RME-1 function, we tested the ability of mCherry-RME-1 lacking the YPSL tail (mCherry-RME-1ΔYPSL) to rescue *rme-1(b1045)* mutants. The expression of mCherry-RME-1(+) or mCherry-RME-1(ΔYPSL) in *rme-1* null mutants fully rescued the formation of abnormal recycling endosome (RE) vacuoles containing accumulated basolaterally recycling fluid (Figure 7E), indicating that the interaction of RME-1 with ALX-1 is not required for fluid recycling. In stark contrast, we found that the expression of mCherry-RME-1(+), but not mCherry-RME-1(ΔYPSL), rescued the abnormal intracellular accumulation of hTAC-GFP and the abnormal localization and/or morphology of GFP-SDPN-1 (Figure 7F; Figure S7). The failure of mCherry-RME-1(ΔYPSL) to rescue these phenotypes suggests that RME-1's function in SDPN-1 recruitment and hTAC recycling requires interaction with ALX-1.

In a similar set of experiments, we compared the ability of mCherry-ALX-1 or mCherry-ALX-1 lacking the C-terminal NPF tripeptide (mCherry-ALX-1ΔNPF) to rescue *alx-1* mutant phenotypes. Interestingly, we found that mCherry-ALX-1(ΔNPF) fully rescued *alx-1(gk275)* phenotypes associated with MVEs and late endosomes, including the abnormal increase in the number of GFP-HGRS-1-labeled endosomes and the size and/or morphology defects in LMP-1-GFP-labeled late endosomes (Figures 7G and 7H; Figure S8). These results further confirm that RME-1 is not required for these functions of ALX-1. By contrast, mCherry-ALX-1(ΔNPF) could not rescue the recycling associated phenotypes of *alx-1* mutants, including hTAC-GFP accumulation or basolateral recruitment of GFP-SDPN-1 (Figure 7H; Figure S8). As expected, mCherry-ALX-1(+) rescued both the MVE- and/or late-endosome- and RE-associated phenotypes of *alx-1* mutants (Figures 7G and 7H; Figure S8). These results genetically separate the functions of ALX-1, indicating that the effects of *alx-1* mutants on hTAC and SDPN-1 are through RME-1 on recycling endosomes and are not indirect effects produced by defective MVEs or late endosomes.

Discussion

In this study, we show for the first time that an Alix/Bro1p family member functions in the endocytic recycling pathway, in association with the recycling endosome regulator RME-1. We also show that ALX-1 is required for the degradation of membrane proteins in *C. elegans*, likely functioning with the ESCRT machinery in the multivesicular endosome, as is thought to be the case for other members of the Alix/Bro1p family [7]. Consistent with our previous studies showing that RME-1 does not function in early or late endosomes, we found that RME-1 does not colocalize with HGRS-1-positive MVEs in the intestine, and *rme-1* null mutants display normal degradation of membrane proteins in early

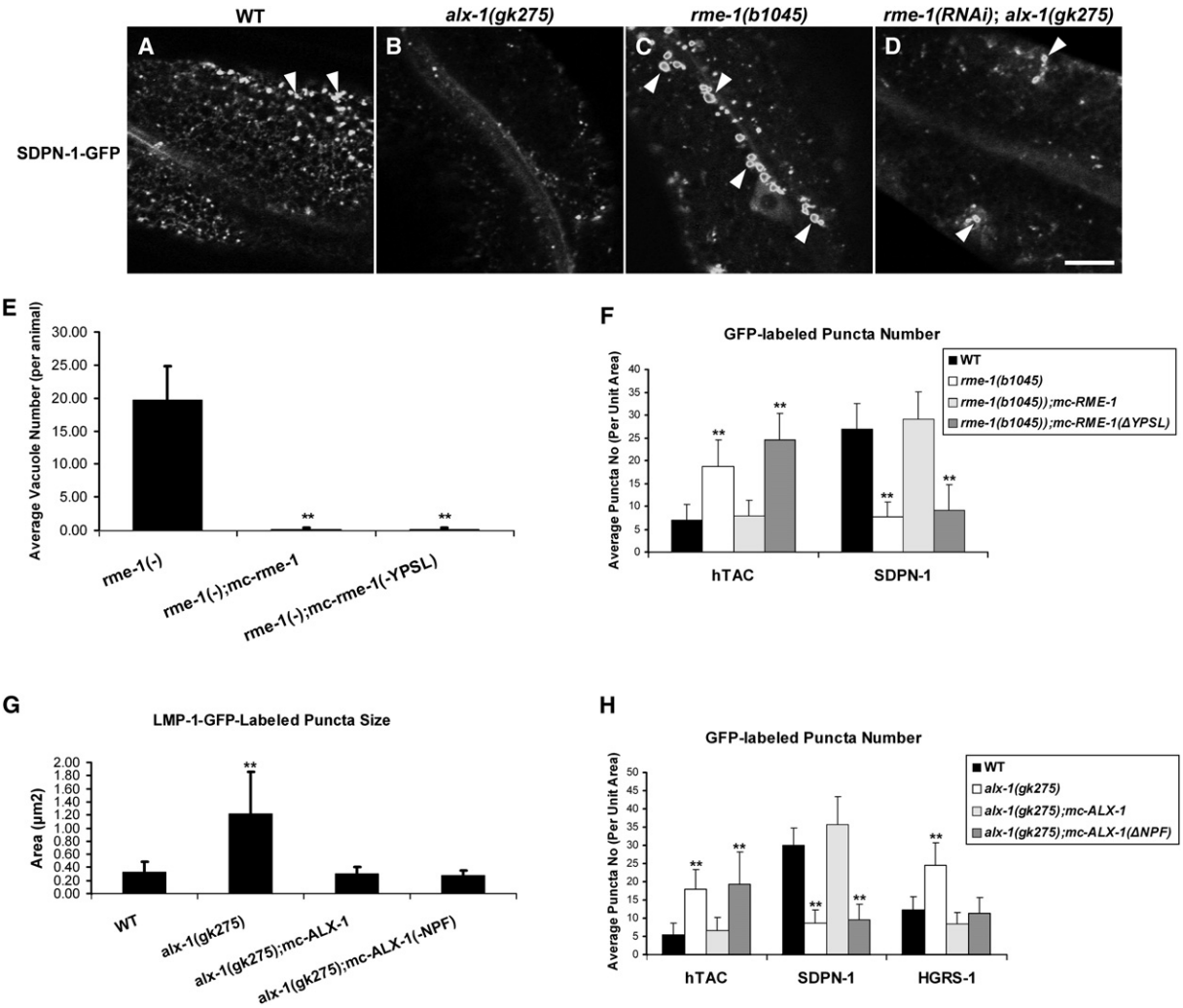

Figure 7. Genetic Separation of Protein Functions in Endocytic Transport Pathways

(A–D) Syndapin/SDPN-1-GFP localization is abnormal in *alx-1* mutant and *rme-1* mutant intestinal cells. Arrowheads indicate endosomes labeled by SDPN-1-GFP. The scale bar represents 10 μm.

(A) Confocal images of wild-type animals show abundant SDPN-1-GFP-labeled basolateral punctate and tubular endosomes.

(B) In *alx-1* mutant animals, most basolateral SDPN-1-GFP-positive structures are missing, and most of the remaining SDPN-1-GFP signal appears diffuse.

(C) In *rme-1* mutant animals, basolateral SDPN-1-GFP-labeled structures are fewer, and many of those that remain are enlarged.

(D) *alx-1(gk275);rme-1(RNAi)* animals lack most basolateral SDPN-1-GFP-labeled structures like *alx-1* mutant animals, but the remaining structures appear enlarged.

(E–H) Rescue experiments genetically separate ALX-1 functions and indicate a requirement for the ALX-1/RME-1 interaction in vivo. Interaction-defective mutant forms of RME-1 (ΔYPSL) or ALX-1 (ΔNPF), expressed as mCherry (MC) fusions, were compared to wild-type forms in their ability to rescue specific *rme-1(b1045)* or *alx-1(gk275)* mutant phenotypes in the intestine. One set of phenotypes that was assayed focused on recycling endosomes: the abnormal accumulation of basolaterally recycling pseudocoelomic fluid in enlarged vacuoles-REs, intracellular recycling cargo hTAC-GFP accumulation, and basolateral SDPN-1-GFP recruitment and/or morphology. In addition, ALX-1(ΔNPF) was compared to intact ALX-1 in its ability to rescue *alx-1* mutant-associated defects in the degradative pathway: multivesicular endosome number, as assayed by GFP-HGRS-1, and late-endosome size, as assayed by LMP-1-GFP.

(E) The expression of either mCherry (MC)-tagged RME-1 or MC-tagged RME-1(ΔYPSL) rescues basolateral fluid accumulation in *rme-1(b1045)* mutants. Error bars represent the standard deviations from the mean (n = 10 each).

(F) The last two bars in each group show the relative degree of rescue of *rme-1(b1045)* mutant defects achieved by expression of MC-tagged RME-1 or MC-tagged RME-1(ΔYPSL). Note that wild-type MC-RME-1 rescues both defects, whereas MC-RME-1(ΔYPSL) cannot rescue the *rme-1(b1045)*-associated defects.

(G and H) The last two bars in each graph show the relative degree of rescue of *alx-1(gk275)* mutant defects achieved by expression of MC-tagged ALX-1 or MC-tagged ALX-1(ΔNPF). Note that wild-type MC-ALX-1 rescues all defects, whereas MC-ALX-1(ΔNPF) can only rescue *alx-1*-associated phenotypes of the degradative pathway, LMP-1-GFP endosome size (G), and GFP-HGRS-1 puncta number (H) but cannot rescue phenotypes associated with the recycling pathway, hTAC-GFP, and SDPN-1-GFP puncta number (H). Asterisks indicate a significant difference in the one-tailed Student's t test ($p < 0.01$).

embryos. In addition, *rme-1* mutants display normal HGRS-1-labeled MVE morphology and number in the intestine. Thus, our studies indicate a dual requirement for ALX-1 in both the recycling and degradative pathways, whereas RME-1 is specific for recycling.

Previous studies indicated that mammalian Alix facilitates virus budding from the plasma membrane of infected cells through direct binding to the sequence motif YPXL within viral Gag protein late-budding domains [18–20]. Similarly, the *Aspergillus* Alix/Bro1p homolog PalA interacts with its partner protein PacC through YPXL motifs [21]. Our studies indicate an important interaction between the central region of ALX-1 and a C-terminal YPSL sequence in RME-1. In addition, the C-terminal NPF sequence in ALX-1 contributes to the interaction between ALX-1 and RME-1, presumably through the NPF-binding pocket present in the EH domain. The NPF-mediated interaction between ALX-1 and RME-1 is required for the function of ALX-1 in recycling but appears to be dispensable for ALX-1 function in MVEs and/or late endosomes. This genetic separation of the two functions of ALX-1 indicates mechanistic differences between ALX-1's roles in these two aspects of endocytic transport.

Consistent with a dual function for ALX-1 in vivo, we found evidence for ALX-1 localization to both types of endocytic organelles, the HGRS-1-positive MVE and the RME-1-positive recycling endosomes. Interestingly, recent studies in human T cells and macrophages using quantitative electron microscopy (EM) methods revealed an enrichment of endogenous human Alix on tubular-vesicular endosomal membranes containing transferrin, consistent with the residence of human Alix on recycling endosomes [49]. Alix siRNA in HeLa cells was reported not to affect transferrin recycling but did affect endosome morphology [25]. In this study, we found that the expression of dominant-negative Alix in HeLa cells dramatically interfered with MHC class I recycling but did not significantly affect transferrin recycling, suggesting that the role of Alix in recycling cargo endocytosed independently of clathrin is a conserved function. We note, however, that the interaction sites that we identified between *C. elegans* RME-1 and ALX-1 do not seem to be conserved in their human homologs. Similarly, although human syndapin binds to Ehd1/mRme-1 directly, and worm SDPN-1 appears to function with RME-1 in recycling, the NPF-containing sequences in syndapin I and II recognized by Ehd1 are lacking in Ce-SDPN-1. Thus, although our results suggest that these proteins function together in worms and mammals, the binding modes among those proteins might have been shuffled during metazoan evolution.

In yeast, the ALX-1 homolog Bro1p is required at the limiting membrane of specialized MVEs [7] for the sorting of monoubiquitinated membrane proteins into lumenal vesicles and productive transport to the vacuole [8]. However, some controversy remains over the requirement for Alix in MVE-mediated degradation of membrane proteins because Alix-depleted HeLa cells were not delayed in the degradation of EGF receptors [25]. Alix is clearly required for the budding of retroviruses in mammals, another transport process that utilizes the MVE/ESCRT machinery [12, 18–20]. In *C. elegans alx-1* mutants, we observed defects in intestinal MVE and/or late-endosome morphology and a very significant delay in the degradation of endocytosed membrane proteins CAV-1-GFP and RME-2-GFP in embryos, indicating the conservation of this function in nematodes. Consistent with our results, Shaye and Greenwald [50] reported that the degradation of LIN-12/Notch receptors in vulval precursor cells is delayed in animals depleted of ALX-1 by RNAi methods. Although there are no previously known mechanistic links between the degradative and recycling branches of the endocytic pathway, it might be advantageous for the cell to coordinate transport through multiple branches in the pathway, perhaps allowing a coordinated response to changes in cargo type, overall cargo load, and/or the local cellular environment.

Although RME-1/mRme-1/Ehd1 is required for the efficient recycling of cargo internalized by clathrin-dependent and clathrin-independent mechanisms [30, 31, 38, 41], our results suggest that ALX-1 is specifically required to recycle cargo of the clathrin-independent class. Consistent with this functional difference, not all basolateral RME-1-positive structures appear positive for ALX-1. Also, basolateral fluid recycling, which can probably utilize either RME-1-dependent recycling pathway, does not appear to require the RME-1/ALX-1 interaction.

Although the mechanisms controlling the recycling of clathrin-independent cargo remain poorly defined, it is clear that local actin dynamics on endosomal membranes are important for productive transport of such cargo from recycling endosomes to the plasma membrane. For instance the inhibition of actin polymerization with drugs such as latrunculin A or cytochalasin D specifically disrupts recycling of clathrin-independent cargo in HeLa cells such as MHC class I and Tac, whereas under the same conditions, the clathrin-dependent cargo transferrin recycles normally [44, 51, 52]. Likewise, the membrane-associated actin regulator Arf6 is required to recycle clathrin-independent but not clathrin-dependent cargos [5]. Interestingly, the knockdown of Alix in HeLa cells is known to perturb intracellular actin distribution, and Alix has been reported to copurify with cytoskeleton components, suggesting a possible functional link between Alix family proteins and membrane-associated actin dynamics [23–25]. Syndapin is known to facilitate the recruitment of N-WASP to membranes, thus activating Arp2/3-directed actin branching and polymerization [53, 54]. We found that *alx-1* mutants showed greatly reduced recruitment of SDPN-1/syndapin to basolateral endosomes, suggesting that ALX-1 promotes recycling through SDPN-1/syndapin and possibly N-WASP and the Arp2/3 machinery. Because actin dynamics are thought to promote vesicle scission at the plasma membrane of yeast and mammalian cells, RME-1, ALX-1, and SDPN-1 might act in a similar way to promote endosomal carrier scission.

Supplemental Data

Supplemental Results, Experimental Procedures, eight figures, and one table are available at http://www.current-biology.com/cgi/content/full/17/22/1913/DC1/.

Acknowledgments

We thank J. Donaldson, R. Sadoul, and C. Chatellard-Causse for important reagents. We also thank J. Donaldson, R. Weigert, C. Martin,

P. Schweinsberg, and Z. Pan for their generous advice and technical assistance. This work was supported by National Institutes of Health grant GM67237 to B.D.G.

Received: August 3, 2007
Revised: October 8, 2007
Accepted: October 16, 2007
Published online: November 8, 2007

References

1. Nichols, B. (2003). Caveosomes and endocytosis of lipid rafts. J. Cell Sci. *116*, 4707–4714.
2. Gesbert, F., Sauvonnet, N., and Dautry-Varsat, A. (2004). Clathrin-independent endocytosis and signalling of interleukin 2 receptors IL-2R endocytosis and signalling. Curr. Top. Microbiol. Immunol. *286*, 119–148.
3. Mukherjee, S., Ghosh, R.N., and Maxfield, F.R. (1997). Endocytosis. Physiol. Rev. *77*, 759–803.
4. Maxfield, F.R., and McGraw, T.E. (2004). Endocytic recycling. Nat. Rev. Mol. Cell Biol. *5*, 121–132.
5. Naslavsky, N., Weigert, R., and Donaldson, J.G. (2004). Characterization of a nonclathrin endocytic pathway: Membrane cargo and lipid requirements. Mol. Biol. Cell *15*, 3542–3552.
6. Katoh, K., Shibata, H., Suzuki, H., Nara, A., Ishidoh, K., Kominami, E., Yoshimori, T., and Maki, M. (2003). The ALG-2-interacting protein Alix associates with CHMP4b, a human homologue of yeast Snf7 that is involved in multivesicular body sorting. J. Biol. Chem. *278*, 39104–39113.
7. Odorizzi, G., Katzmann, D.J., Babst, M., Audhya, A., and Emr, S.D. (2003). Bro1 is an endosome-associated protein that functions in the MVB pathway in Saccharomyces cerevisiae. J. Cell Sci. *116*, 1893–1903.
8. Katzmann, D.J., Odorizzi, G., and Emr, S.D. (2002). Receptor downregulation and multivesicular-body sorting. Nat. Rev. Mol. Cell Biol. *3*, 893–905.
9. Gruenberg, J., and Stenmark, H. (2004). The biogenesis of multivesicular endosomes. Nat. Rev. Mol. Cell Biol. *5*, 317–323.
10. Bateman, A., Birney, E., Cerruti, L., Durbin, R., Etwiller, L., Eddy, S.R., Griffiths-Jones, S., Howe, K.L., Marshall, M., and Sonnhammer, E.L. (2002). The Pfam protein families database. Nucleic Acids Res. *30*, 276–280.
11. Kim, J., Sitaraman, S., Hierro, A., Beach, B.M., Odorizzi, G., and Hurley, J.H. (2005). Structural basis for endosomal targeting by the Bro1 domain. Dev. Cell *8*, 937–947.
12. Fisher, R.D., Chung, H.Y., Zhai, Q., Robinson, H., Sundquist, W.I., and Hill, C.P. (2007). Structural and biochemical studies of ALIX/AIP1 and its role in retrovirus budding. Cell *128*, 841–852.
13. Odorizzi, G. (2006). The multiple personalities of Alix. J. Cell Sci. *119*, 3025–3032.
14. Katoh, K., Shibata, H., Hatta, K., and Maki, M. (2004). CHMP4b is a major binding partner of the ALG-2-interacting protein Alix among the three CHMP4 isoforms. Arch. Biochem. Biophys. *421*, 159–165.
15. Gavin, A.C., Bosche, M., Krause, R., Grandi, P., Marzioch, M., Bauer, A., Schultz, J., Rick, J.M., Michon, A.M., Cruciat, C.M., et al. (2002). Functional organization of the yeast proteome by systematic analysis of protein complexes. Nature *415*, 141–147.
16. Schmidt, M.H., Hoeller, D., Yu, J., Furnari, F.B., Cavenee, W.K., Dikic, I., and Bogler, O. (2004). Alix/AIP1 antagonizes epidermal growth factor receptor downregulation by the Cbl-SETA/CIN85 complex. Mol. Cell. Biol. *24*, 8981–8993.
17. Chatellard-Causse, C., Blot, B., Cristina, N., Torch, S., Missotten, M., and Sadoul, R. (2002). Alix (ALG-2-interacting protein X), a protein involved in apoptosis, binds to endophilins and induces cytoplasmic vacuolization. J. Biol. Chem. *277*, 29108–29115.
18. Strack, B., Calistri, A., Craig, S., Popova, E., and Gottlinger, H.G. (2003). AIP1/ALIX is a binding partner for HIV-1 p6 and EIAV p9 functioning in virus budding. Cell *114*, 689–699.
19. von Schwedler, U.K., Stuchell, M., Muller, B., Ward, D.M., Chung, H.Y., Morita, E., Wang, H.E., Davis, T., He, G.P., Cimbora, D.M., et al. (2003). The protein network of HIV budding. Cell *114*, 701–713.
20. Martin-Serrano, J., Yarovoy, A., Perez-Caballero, D., and Bieniasz, P.D. (2003). Divergent retroviral late-budding domains recruit vacuolar protein sorting factors by using alternative adaptor proteins. Proc. Natl. Acad. Sci. USA *100*, 12414–12419.
21. Vincent, O., Rainbow, L., Tilburn, J., Arst, H.N., Jr., and Penalva, M.A. (2003). YPXL/I is a protein interaction motif recognized by aspergillus PalA and its human homologue, AIP1/Alix. Mol. Cell. Biol. *23*, 1647–1655.
22. Matsuo, H., Chevallier, J., Mayran, N., Le Blanc, I., Ferguson, C., Faure, J., Blanc, N.S., Matile, S., Dubochet, J., Sadoul, R., et al. (2004). Role of LBPA and Alix in multivesicular liposome formation and endosome organization. Science *303*, 531–534.
23. Pan, S., Wang, R., Zhou, X., He, G., Koomen, J., Kobayashi, R., Sun, L., Corvera, J., Gallick, G.E., and Kuang, J. (2006). Involvement of the conserved adaptor protein Alix in actin cytoskeleton assembly. J. Biol. Chem. *281*, 34640–34650.
24. Schmidt, M.H., Chen, B., Randazzo, L.M., and Bogler, O. (2003). SETA/CIN85/Ruk and its binding partner AIP1 associate with diverse cytoskeletal elements, including FAKs, and modulate cell adhesion. J. Cell Sci. *116*, 2845–2855.
25. Cabezas, A., Bache, K.G., Brech, A., and Stenmark, H. (2005). Alix regulates cortical actin and the spatial distribution of endosomes. J. Cell Sci. *118*, 2625–2635.
26. Fares, H., and Grant, B. (2002). Deciphering endocytosis in Caenorhabditis elegans. Traffic *3*, 11–19.
27. Grant, B., and Hirsh, D. (1999). Receptor-mediated endocytosis in the Caenorhabditis elegans oocyte. Mol. Biol. Cell *10*, 4311–4326.
28. Grant, B.D., and Sato, M. Intracellular trafficking (January 21, 2006). In WormBook, ed. The *C. elegans* Research Community, WormBook, doi/10.1895/wormbook.1.77.1 (http://www.wormbook.org).
29. Fares, H., and Greenwald, I. (2001). Genetic analysis of endocytosis in Caenorhabditis elegans: Coelomocyte uptake defective mutants. Genetics *159*, 133–145.
30. Grant, B., Zhang, Y., Paupard, M.C., Lin, S.X., Hall, D.H., and Hirsh, D. (2001). Evidence that RME-1, a conserved C. elegans EH-domain protein, functions in endocytic recycling. Nat. Cell Biol. *3*, 573–579.
31. Lin, S.X., Grant, B., Hirsh, D., and Maxfield, F.R. (2001). Rme-1 regulates the distribution and function of the endocytic recycling compartment in mammalian cells. Nat. Cell Biol. *3*, 567–572.
32. Naslavsky, N., and Caplan, S. (2005). C-terminal EH-domain-containing proteins: Consensus for a role in endocytic trafficking, EH? J. Cell Sci. *118*, 4093–4101.
33. Santolini, E., Salcini, A.E., Kay, B.K., Yamabhai, M., and Di Fiore, P.P. (1999). The EH network. Exp. Cell Res. *253*, 186–209.
34. Page, L.J., Sowerby, P.J., Lui, W.W., and Robinson, M.S. (1999). Gamma-synergin: An EH domain-containing protein that interacts with gamma-adaptin. J. Cell Biol. *146*, 993–1004.
35. de Beer, T., Hoofnagle, A.N., Enmon, J.L., Bowers, R.C., Yamabhai, M., Kay, B.K., and Overduin, M. (2000). Molecular mechanism of NPF recognition by EH domains. Nat. Struct. Biol. *7*, 1018–1022.
36. Braun, A., Pinyol, R., Dahlhaus, R., Koch, D., Fonarev, P., Grant, B.D., Kessels, M.M., and Qualmann, B. (2005). EHD proteins associate with syndapin I and II and such interactions play a crucial role in endosomal recycling. Mol. Biol. Cell *16*, 3642–3658.
37. Puffer, B.A., Parent, L.J., Wills, J.W., and Montelaro, R.C. (1997). Equine infectious anemia virus utilizes a YXXL motif within the late assembly domain of the Gag p9 protein. J. Virol. *71*, 6541–6546.
38. Chen, C.C., Schweinsberg, P.J., Vashist, S., Mareiniss, D.P., Lambie, E.J., and Grant, B.D. (2006). RAB-10 is required for endocytic recycling in the Caenorhabditis elegans intestine. Mol. Biol. Cell *17*, 1286–1297.
39. Roudier, N., Lefebvre, C., and Legouis, R. (2005). CeVPS-27 is an endosomal protein required for the molting and the endocytic trafficking of the low-density lipoprotein receptor-related protein 1 in Caenorhabditis elegans. Traffic *6*, 695–705.
40. Yu, X., Odera, S., Chuang, C.H., Lu, N., and Zhou, Z. (2006). C. elegans Dynamin mediates the signaling of phagocytic

receptor CED-1 for the engulfment and degradation of apoptotic cells. Dev. Cell *10*, 743–757.

41. Caplan, S., Naslavsky, N., Hartnell, L.M., Lodge, R., Polishchuk, R.S., Donaldson, J.G., and Bonifacino, J.S. (2002). A tubular EHD1-containing compartment involved in the recycling of major histocompatibility complex class I molecules to the plasma membrane. EMBO J. *21*, 2557–2567.
42. Yamashiro, D.J., and Maxfield, F.R. (1984). Acidification of endocytic compartments and the intracellular pathways of ligands and receptors. J. Cell. Biochem. *26*, 231–246.
43. Burack, M.A., Silverman, M.A., and Banker, G. (2000). The role of selective transport in neuronal protein sorting. Neuron *26*, 465–472.
44. Weigert, R., Yeung, A.C., Li, J., and Donaldson, J.G. (2004). Rab22a regulates the recycling of membrane proteins internalized independently of clathrin. Mol. Biol. Cell *15*, 3758–3770.
45. Naslavsky, N., Weigert, R., and Donaldson, J.G. (2003). Convergence of non-clathrin- and clathrin-derived endosomes involves Arf6 inactivation and changes in phosphoinositides. Mol. Biol. Cell *14*, 417–431.
46. Sadoul, R. (2006). Do Alix and ALG-2 really control endosomes for better or for worse? Biol. Cell *98*, 69–77.
47. Weigert, R., and Donaldson, J.G. (2005). Fluorescent microscopy-based assays to study the role of Rab22a in clathrin-independent endocytosis. Methods Enzymol. *403*, 243–253.
48. Audhya, A., McLeod, I.X., Yates, J.R., and Oegema, K. (2007). MVB-12, a fourth subunit of metazoan ESCRT-I, functions in receptor downregulation. PLoS ONE *2*, e956.
49. Welsch, S., Habermann, A., Jager, S., Muller, B., Krijnse-Locker, J., and Krausslich, H.G. (2006). Ultrastructural analysis of ESCRT proteins suggests a role for endosome-associated tubular-vesicular membranes in ESCRT function. Traffic *7*, 1551–1566.
50. Shaye, D.D., and Greenwald, I. (2005). LIN-12/Notch trafficking and regulation of DSL ligand activity during vulval induction in Caenorhabditis elegans. Development *132*, 5081–5092.
51. Brown, F.D., Rozelle, A.L., Yin, H.L., Balla, T., and Donaldson, J.G. (2001). Phosphatidylinositol 4,5-bisphosphate and Arf6-regulated membrane traffic. J. Cell Biol. *154*, 1007–1017.
52. Radhakrishna, H., and Donaldson, J.G. (1997). ADP-ribosylation factor 6 regulates a novel plasma membrane recycling pathway. J. Cell Biol. *139*, 49–61.
53. Qualmann, B., and Kelly, R.B. (2000). Syndapin isoforms participate in receptor-mediated endocytosis and actin organization. J. Cell Biol. *148*, 1047–1062.
54. Kessels, M.M., and Qualmann, B. (2004). The syndapin protein family: Linking membrane trafficking with the cytoskeleton. J. Cell Sci. *117*, 3077–3086.